



SiliconPV: 17-20 April 2011, Freiburg, Germany

## Investigation of degradation in solar cells from different mc-Si materials

J. Junge<sup>a,\*</sup>, A. Herguth<sup>a</sup>, G. Hahn<sup>a</sup>, D. Kreßner-Kiel<sup>b</sup>, R. Zierer<sup>b</sup>

<sup>a</sup>University of Konstanz, Department of Physics, P.O. Box X916, 78457 Konstanz, Germany

<sup>b</sup>Institute for Experimental Physics, TU Bergakademie Freiberg, Leipziger Str. 23, 09596 Freiberg, Germany

---

### Abstract

The impact of light induced degradation on small lab-type 2x2 cm<sup>2</sup> solar cells made from standard p-type mc-Si material is compared to the degradation of lowly compensated UMG material on the one hand and intentionally Fe and Fe/Cu contaminated material (several ppma of Fe or Fe and Cu are introduced into the melt of electronic grade feedstock before ingot casting) on the other hand. The material is taken from three different ingot heights (bottom, middle and top), respectively. All cells are annealed at 200°C in the dark for several minutes before they are exposed to one sun illumination and the development of the electrical parameters over time is determined. The reference and UMG material behave as expected and show a degradation which is correlated to the boron and interstitial oxygen concentration over the ingot height and therefore can be attributed to B-O related defects. The intentionally Fe and Cu contaminated samples in contrast show a degradation behavior that is more probably correlated to the distribution of the Fe and Cu contamination, as the absolute degradation towards the top of the ingot is higher for highly contaminated material (20 ppma Fe) than in the reference material and the observed time constants for degradation are different. Fe/Cu contaminated material exhibits too low cell performance in the top and bottom part of the ingot to show any significant degradation effects. The lowly contaminated material (2 ppma Fe) behaves like the reference material as long as the wafer material does not contain additional contaminants originating from the crucible walls. Material from near the crucible wall by contrast shows a stronger light induced degradation.

© 2011 Published by Elsevier Ltd. Open access under [CC BY-NC-ND license](https://creativecommons.org/licenses/by-nc-nd/4.0/).

Selection and/or peer-review under responsibility of SiliconPV 2011

mc-Si; degradation

---

\* Corresponding author. Tel.: +49 7531 88 2082 ; fax: +49 7531 88 3895 .

E-mail address: [johannes.junge@uni-konstanz.de](mailto:johannes.junge@uni-konstanz.de).

## 1. Purpose of the work

The Light Induced Degradation (LID) in multicrystalline (mc) silicon (Si) material has been detected mainly in highly doped materials [1] or in material of very high quality [2]. But as the material quality of standard mc-Si material is continuously increasing, LID of mc-Si might become more and more important. In addition, highly doped but partially compensated Upgraded Metallurgical Grade (UMG) silicon has entered the market although recent publications indicate that only the net doping concentration is relevant for LID [3], [4]. In contrast to Czochralski (Cz) Si there are many other impurities present in mc-Si and the question arises if the materials suffer from other degradation effects except from the well known B-O correlated degradation. One candidate is degradation due to the release of interstitial iron ( $Fe_i$ ) from FeB pairs which is also known to decrease the minority carrier lifetime and thus the cell performance [5]. A similar effect involving other transition metals (e.g. Cu, Cr) also seems to be possible.

## 2. Experiment

The solar cells are fabricated according to a simple photolithography-based lab-type process on different materials [6]. They include lowly compensated UMG-Si material as well as intentionally Fe and Cu contaminated mc-Si material where several ppm (2 or 20) of these transition metals were introduced into the melt of electronic grade feedstock before ingot casting. Standard mc-Si material is processed and characterized for reference. Apart from the different materials, also different ingot positions are investigated in the mc materials, as impurities are unevenly distributed over the ingot height due to segregation. The influence of contaminants from the crucible wall is also investigated. The degradation is determined after annealing in darkness at 200°C for 6 min. The annealing conditions are a compromise to anneal on the one hand the B-O complex [7] and on the other hand to maintain most of the FeB pairs which are already dissolving at this temperature, but are expected to repair to a large extent during the (slow) cooling process [8]. The illuminated IV parameters are determined using standard test conditions directly after the annealing and again after 14 h of illumination at 1 sun and 25°C. The temporal behaviour of the degradation is determined after a second anneal and continuous monitoring of  $V_{oc}$  during an illumination of about 1 sun in a special measurement setup again at 25°C.

## 3. Results

### 3.1. Defect and dopant distributions for the different ingots

The impurity distribution of [Fe] and [Cu] in the investigated ingots (Fig. 1) is obtained via Neutron Activation Analysis (NAA) from the as grown material. Fourier Transformed Infrared Spectroscopy (FTIR) is applied to obtain the interstitial oxygen concentration [ $O_i$ ] (Fig. 2, left side). The dopant concentration (Fig. 2, right side) is determined via resistivity measurements for the reference and the contaminated materials. They are therefore to be considered as upper limits for the boron concentration [B] as other dopants could as well decrease the resistivity. The UMG ingot was characterized using a combination of FTIR spectroscopy and Hall measurements [9] which allow to determine [P] and [B] in the material. As for LID only the net dopant concentration  $p_0 = [B] - [P]$  seems to be of importance [3],[4] this value is depicted in Fig. 2 (right side) for the UMG material. The graph shows a nearly tenfold increased dopant concentration for the UMG material in the bottom and middle of the ingot compared to the reference and the contaminated materials. Thus the resistivity of the investigated materials varies between 0.2 and 1  $\Omega\text{cm}$ .

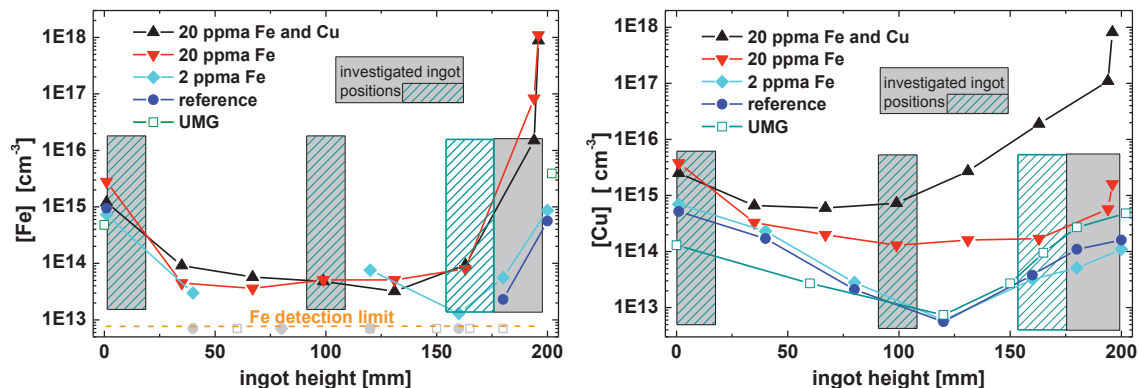


Fig. 1. Height distribution of [Fe] (left) and [Cu] (right) for the investigated materials (as grown). The approximated positions where the material for solar cell processing is taken from are marked in grey (or shaded green for the UMG material).

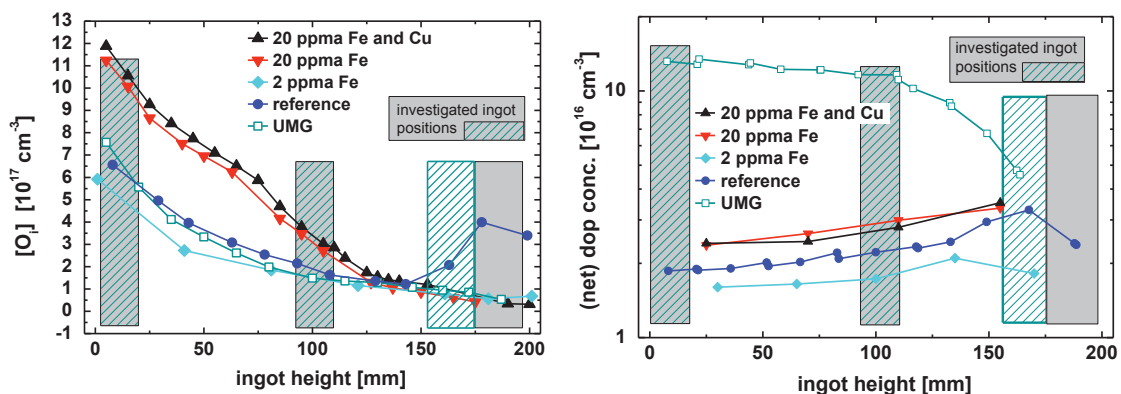


Fig. 2.  $[O_i]$  (left) and (net) dopant concentration (right) of the different investigated materials over the ingot height (as grown).

### 3.2. Long term degradation

The degradation of the UMG material correlates with the decreasing  $[O_i]$  from the bottom towards the transition point of the ingot. Together with the high net doping (about one order of magnitude higher in UMG than in the other materials) the long term degradation can clearly be attributed to the formation of B-O complexes (Table 1). A similar trend can be observed in the reference and 2 ppma Fe contaminated materials, although on much smaller scale as the dopant concentration is much lower in these materials. The highly Fe and Fe/Cu contaminated materials by contrast show the strongest degradation in the middle or the top region of the ingot although  $[O_i]$  at the bottom is very high in these materials (Fig. 2, left side), which should greatly enhance B-O degradation as the concentration of B-O defects depends approximately quadratically on  $[O_i]$  [10]. This unexpected result might be due to the significantly higher concentration of transition metals in the middle and top region compared to the reference and also due to the better performance of solar cells from middle and top region which makes them more sensitive to degradation effects.

Table 1. Selected  $J_{sc}$  and  $V_{oc}$  values of different mc Si solar cells before and after degradation from different ingot positions (bottom (b), middle (m), top (or before transition point for UMG) (t)).

Material and position	Initial values		Degradation		[B], [net dop.]	[O <sub>i</sub> ]
	$j_{sc}$ [mA/cm <sup>2</sup> ]	$V_{oc}$ [mV]	$\Delta j_{sc}$ [%]	$\Delta V_{oc}$ [%]	[10 <sup>16</sup> at/cm <sup>3</sup> ]	[10 <sup>17</sup> at/cm <sup>3</sup> ]
UMG b	28.8	620.5	7.5	1.6	13	7.5
UMG m	31.2	627.2	2.3	0.4	11.6	1.5
UMG t	32.1	616.3	0.9	0.4	1	1
Reference b	32.1	610.5	1.3	0.6	1.9	6.6
Reference m	33.2	626.2	0.6	0.3	2.2	1.9
Reference t	28.0	593.1	0.4	0	2.4	3.6
Fe (20 ppma) b	25.4	585.0	0.4	0.2	2.4	11
Fe (20 ppma) m	32.2	628.6	1.9	0.7	2.6	3.2
Fe (20 ppma) t	29.1	604.8	0.7	0.4	3.5	0.5
Fe/Cu (20 ppma) m	30.8	611.4	2.0	0.7	2.5	3.4

### 3.3. Time resolved measurements

The time resolved degradation measurement reveals the different time scales in which the degradation takes place and thus indicates different degradation mechanisms. The UMG and the reference material show a relatively slow decrease in  $V_{oc}$  which saturates after several hours of illumination at 1 sun and a temperature of 25°C.

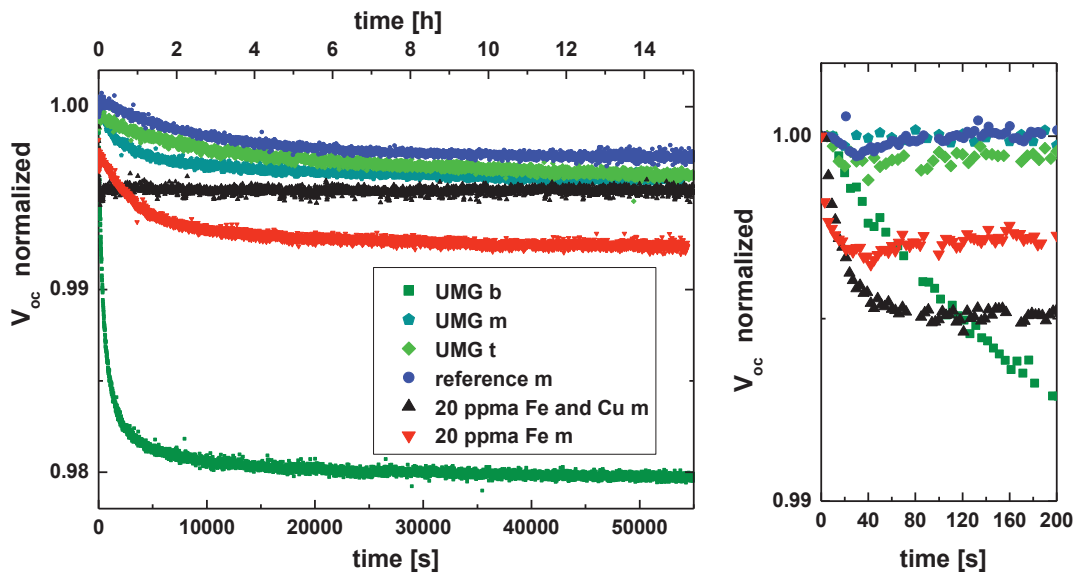


Fig. 3. Time resolved evolution of the  $V_{oc}$  decay of solar cells made from different materials under 1 sun illumination at 25°C. The left side shows the decay for all materials during 14 h of illumination at 1 sun. The very fast decay for Fe and Fe/Cu contaminated material (originating from the middle of the respective ingot) is depicted on the right side (same data but different time scale).

This behavior can clearly be attributed to B-O degradation. The highly Fe and Fe/Cu contaminated samples by contrast show a significant decrease of  $V_{oc}$  during the first minute of illumination. While the Fe contaminated sample additionally shows a B-O related degradation over several hours, the Fe/Cu contaminated sample only exhibits the short term degradation and remains stable afterwards. Probably due to the lower bulk lifetime in this sample, recombination due to B-O complexes is not limiting [11] and thus B-O degradation not observable.

To gain further information on the nature of the observed fast degradation, the annealing conditions were adapted. Degraded samples (after 14h @ 1sun and 25°C) were annealed for 10 min at 40°C in the dark. This should reverse a FeB-type degradation but should not significantly affect the degradation due to the B-O defects. Comparisons to short term degradations of the same cells after an anneal step at 200°C showed the same decay behavior (Fig. 4, left side) and thus indicate a FeB type defect.

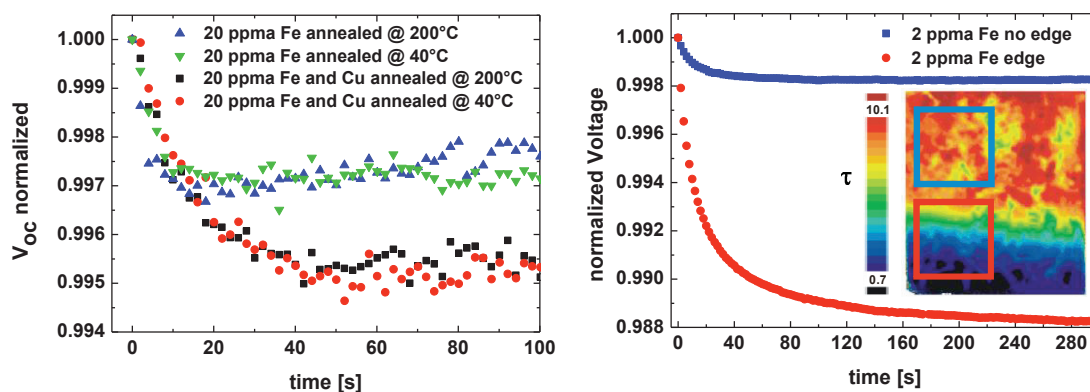


Fig. 4. Time resolved degradation of Fe/Cu and Fe contaminated material after different annealing steps (left) and influence of the crucible wall on degradation (right). The origin of the investigated test cells is marked in the inserted lifetime map of the as grown wafer and colors are analogous to the graph's colors.

The difference between the highly Fe and highly Fe/Cu contaminated sample (Fig. 4.) might be explained by (i) CuB defect formation [12], (ii) a locally increased  $[Fe_i]$  which might be possible because of the small sample size or (iii) the different material quality which leads to different injection levels at 1 sun illumination and thus a different response of the samples to the  $Fe_i$  related defect [5].

Similar short term degradation is observed for samples originating from close to the crucible edge of an ingot which was slightly contaminated with 2 ppma Fe (right side of Fig. 4). While there is only a negligible degradation visible on material which originates from a position further away from the edge, the cell which is prepared from edge-affected material even shows a more severe short term degradation than the samples presented on the left side of Fig. 4. The comparable temporal behavior suggests a similar defect type. The curves (Fig. 4, right side) are much smoother because in this case the degradation was not light induced but current induced (light induced measurements show qualitatively the same behavior). The larger time constants compared to Fig. 4, left side might be due to the lower current injection for these measurements (corresponding to about 0.25-0.5 suns).

#### 4. Conclusions

B-O related LID is visible in state of the art mc-Si material but only shows significant negative influence if the net dopant concentration is relatively high and coincides with high  $[O_i]$ , as expected. Additionally, high contamination with transition metals like Fe and Cu can lead to a second form of degradation which takes place within less than a minute after a moderate annealing step (or several hours storage in the dark at room temperature). The edge of an ingot exhibits a similar short term degradation behavior suggesting that the low material quality next to the crucible wall is (at least partially) due to transition metals like Fe and Cu.

#### Acknowledgements

The underlying project of this report was financially supported by the German Federal Ministry for the Environment, Nature Conservation and Nuclear Safety and all the industry partners within the research cluster SolarFocus (0327650 H). The financial support from the BMU project 0325079 is also gratefully acknowledged, in particular for the processing and characterization equipment. The NAA results and resistivity data were provided by Isolde Reis, coordinator of the SolarFocus project. The content of this publication is the responsibility of the authors.

#### References

- [1] De Wolf S, Choulat P, Szlufcik J, Perichaud I, Martinuzzi S, Hassler C et al. Light-induced degradation of very low resistivity multi-crystalline silicon solar cells. *Proc. 28<sup>th</sup> IEEE PVSC*, Anchorage 2000, p. 53–6.
- [2] Damiani B, Nakayashiki K, Kim DS, Yelundur V, Ostapenko S, Tarasov I et al. Light induced degradation in promising multi-crystalline silicon materials for solar cell fabrication. *Proc. 3<sup>rd</sup> WCPEC*, Osaka 2003, p. 927–30.
- [3] Kopecek R, Arumughan J, Peter K, Good EA, Libal J, Acciarri M et al. Crystalline Si solar cells from compensated material: behaviour of light induced degradation. *Proc. 23<sup>rd</sup> EU PVSEC*, Valencia: 2008, p. 1855-8.
- [4] Voronkov VV, Falster R, Latent complexes of interstitial boron and oxygen dimers as a reason for degradation of silicon-based solar cells. *J Appl Phys* 2010;**107**:053509.
- [5] Schmidt J. Effect of dissociation of iron-boron pairs in crystalline silicon on solar cell properties. *Progr Photovolt Res Appl* 2005;**13**:325-31.
- [6] Junge J, Herguth A, Seren S, Hahn G, Reducing the impact of metal impurities in block-cast mc silicon, *Proc. 24<sup>th</sup> EUPVSEC*, Hamburg 2009, p. 1131-1136.
- [7] Fischer H, Pschunder W. Investigation of photon and thermal induced changes in silicon solar cells. *10<sup>th</sup> IEEE PVSC*, Palo Alto 1974, p. 404–11.
- [8] Zoth G, Bergholz W. A fast, preparation-free method to detect iron in silicon. *J Appl Phys* 1990;**67**:6764-71.
- [9] Zierer R, Gärtner G, Möller HJ. Determination of dopant concentrations in UMG-silicon by FT-IR spectroscopy, Hall- and resistivity measurements. *Proc. 25<sup>th</sup> EU PVSEC*, Valencia: 2010, p. 1318-21.
- [10] Bothe K, Schmidt J. Electronically activated boron-oxygen-related recombination centers in crystalline silicon. *J Appl Phys* 2006;**99**:013701.
- [11] Bothe K, Sinton R, Schmidt J. Fundamental boron-oxygen-related carrier lifetime limit in mono- and multicrystalline silicon. *Progr Photovolt Res Appl*, 2005;**13**:287-96.
- [12] Aboelfotoh M, Svensson BG. Copper passivation of boron in silicon and boron reactivation kinetics. *Phys Rev B* 1991;**44**:12742-47